AIAA JOURNAL
Vol. 53, No. 5, May 2015

Blast Response of Sandwich Plates with a Compressible Core: Extended High-Order Approach

Y. Frostig*
Technion–Israel Institute of Technology, 32000 Haifa, Israel
and
N. Rodcheuy† and G. A. Kardomateas‡
Georgia Institute of Technology, Atlanta, Georgia 30332-0150

DOI: 10.2514/1.J053309

The transient blast response of a sandwich panel that consists of a compressible core with in-plane rigidity using the extended high-order sandwich panel theory is presented and compared with elasticity closed-form solutions. The mathematical formulation of the extended high-order sandwich panel theory for the transient dynamic response of sandwich plates is described along with a numerical investigation. The extended high-order sandwich panel theory formulation takes into account the shear resistance of the core and its compressibility, which is envisaged through nonidentical displacements of the upper and the lower facesheets and its in-plane rigidity. The equations of motion and the appropriate boundary conditions are derived using the Hamilton's principle. A numerical investigation is conducted on a simply supported sandwich panel, and its results are compared with a benchmark elasticity closed-form solution. The results include deformed shapes at the first millisecond at various time steps; displacements of the various constituents, as well as various stress resultants in the facesheets; and stress distributions within the core and at its interfaces with the facesheets. The extended high-order sandwich panel theory and the elasticity benchmark results correlate very well. Finally, a summary is presented and conclusions are drawn.

Nomenclature

A_j, D_j	=	in-plane and flexural rigidities of facesheets, where j is equal to t, b
a, b	=	length and width of the plate respectively
b_{pxij}, b_{pxij}	=	length and width of loaded area centered at x_i, y_i
c	=	thickness of core
$\mathrm{d}t$	=	time difference
$\mathrm{d}V$	=	volume of a differential segment
$\mathrm{d}x$, $\mathrm{d}y$	=	differential segment length in x and y directions
d_j	=	thickness of facesheets, where j is equal to t, b
E_c, G_{xyc}	=	modulus of elasticity and in-plane shear modulus of core
E_j	=	modulus of elasticity of the facesheets, where j is equal to t, b
$f_{,klnm}$	=	$\partial f/\partial k\partial l\partial m\partial n$ (where k, l, n, m is equal to x, y, z, t); function derivative with respect to various variables
G_{kz}	=	vertical shear moduli of core, where k is equal to x, y
H	=	Heaviside (ramp) function
I_{mj}	=	rotary inertia of facesheets (where j is equal to t, b)
j	=	t, b, c; facesheets and core subscript indices
L	=	Lagrangian
M_j	=	mass of facesheets and core (where j is equal to t, b, c)
M_{klmc}	=	high-order moments in core due to in-plane normal stresses (where k, l is equal to x, y; and m is equal to 2,3)
M_{Qmkc}	=	high-order moments in core due to vertical shear stresses in the core (where k is equal to x, y; and m is equal to 1,2)
N_c	=	number of concentrated loads
N_{klej}, P_{kej}, M_{klej}	=	external loads: in-plane, vertical, and bending moments applied at the edges (where k and l equal to x, y)
N_{klj}, M_{klj}	=	in-plane force and moment resultants due to normal and shear stress of facesheets (where k, l is equal to x, y; and j is equal to t, b)
n_{xj}, n_{yj}, q_j	=	external distributed loads: in-plane (x, y) and vertical loads (where j is equal to t, b)
P_{ij}	=	vertical localized load resultant
Q_{kc}	=	vertical shear stress resultant of core
R_{zzc}, M_{zzc}	=	Force and moment resultants in core due to the vertical normal stresses
t	=	time coordinate
T, U, V	=	kinetic, strain, and potential energies of external loads
t, b, c	=	upper and lower facesheets, and core subscript indices, respectively
$u_{j,t}$, $v_{j,t}$, $w_{j,t}$	=	velocities in the longitudinal, transverse, and vertical directions of the facesheets and core (where j is equal to t, b, c)
u_k, v_k	=	unknown functions of in-plane displacements in x and y directions of core (where (k is equal to 0,1,2,3)
u_{oj}, v_{oj}, w_j	=	longitudinal and transverse in-plane displacements at midheight of facesheets and vertical displacements of the facesheets (where j is equal to t, b)
V_j	=	volume of the upper and lower facesheets and core (where j is equal to t, b, c)
$w_{j,k}$	=	slope of the vertical displacements (where j is equal to t, b; and k is equal to x, y)
w_l	=	vertical displacement unknown's core (where l is equal to 0,1,2)
x, y, z	=	coordinate system
x_e, y_e	=	x and y coordinates of the edges
z_j	=	vertical coordinates of each facesheet and core (where j is equal to t, b, c)

Received 19 January 2014; revision received 23 September 2014; accepted for publication 3 January 2015; published online 6 March 2015.

*Professor, Ashtrom Engineering Company Chair in Civil Engineering, Faculty of Civil and Environmental Engineering; cvrfros@techunix.technion.ac.il (Corresponding Author).
†Graduate Research Assistant, School of Aerospace Engineering.
‡Professor, School of Aerospace Engineering.

α_{kbc} = boundary conditions edge coefficient (where k is equal to x, y)
δ = variational operator
λ_{kj} = Lagrange multiplier in each direction at the upper and lower face–core interfaces (where k is equal to x, y, z; and j is equal to t, b)
μ_{ckl} = Poisson ratio of core various directions (where k and l equal to x, y)
μ_{kl} = Poisson ratio of facesheets in various directions (where k and l equal to x, y; and j is equal to t, b)
ρ_j = density of the upper and lower facesheets and the core (where j is equal to t, b, c)
σ_{iij}, ε_{iij} = longitudinal and transverse normal stresses and strains in facesheets and core (where i is equal to x, y; and j is equal to t, b, c)
σ_{zzc}, ε_{zzc} = vertical normal stresses and strains in the vertical direction of the core
τ_{izc}, γ_{izc} = vertical shear stresses and shear angle in the core (where i is equal to x, y)
τ_{xyj}, γ_{xyj} = in-plane shear stress and shear angle, respectively, at the facesheets and core (where j is equal to t, b, c)
ϕ_x, ϕ_y = slope of x and y sections at core's midheight

Introduction

BLAST loading is always associated with pick displacements and stresses and is described by a transient dynamic response. However, in an ordinary solid plate, that response yields transient vertical displacements in time that are uniform through the depth of the plate. But, in a sandwich panel, these temporal phenomena are associated with different displacement patterns of the facesheet plates. In general, a typical core of a sandwich plate provides shear resistance to the sandwich plate, through the bond of the facesheets with the core. In addition, when loads are applied to the facesheets, the core also serves as a kind of complex elastic foundation, which rests on a deformable foundation, i.e., one of the face sheers. Hence, it has vertical and in-plane rigidities (x and y directions) due to normal stresses involved in addition to the shear resistance.

A typical sandwich panel in aeronautical, naval, or transportation applications consists of two metallic or laminated composite facesheets and a lightweight core that is made of a metallic or Nomex® honeycomb, low-strength foam, or solid lightweight materials, such as balsa wood. In the case of a metallic honeycomb core, its rigidities are assumed to be infinite in the vertical direction with finite shear resistance, whereas its in-plane rigidity is very small. On the other hand, when foam cores or lightweight solid materials are considered, their shear resistance, vertical, and in-plane (x and y directions) rigidities due to normal stresses may be associated with indentations and localized bending in one of the facesheets when localized loads are applied. Please notice that the in-plane rigidities of the core are, in general, small as compared with the couple action of the facesheets. In the case when local bending in the facesheets is involved, such as wrinkling or transient loading schemes, the in-plane rigidity of the core may affect the response.

The classical approaches for the analysis research of sandwich panels may be described by two main categories. The first category assumes that the cores are an antiplane type, i.e., very stiff in the vertical directions and with negligible in-plane rigidity in the longitudinal direction; see Allen [1], Plantema [2], Zenkert [3], and Vinson [4], which are appropriate for the response of a sandwich panel made of a metallic honeycomb core. In general, the response of such a panel is modeled by a panel that assumes that the core is incompressible, such as first-order or high-order shear deformable plate models. They replace the actual layered panel by an equivalent single layer. The second category, denoted as the layered approach, describes the overall response through the interconnection of the three layers (with general displacement patterns) by fulfillment of equilibrium and compatibility conditions at their interfaces (see, for example, the high-order model by Frostig et al. [5] or the works of Carrera and Brischetto [6]) using presumed displacement distribution through the depth of the panel.

The elasticity solutions or similar have been adopted too for the analysis of sandwich panels throughout the years for specific boundary conditions and to mention a few: Pagano [7] solved the response of composite and sandwich panels; Pagano and Hatfield [8] used it for bidirectional composite panels; Zenkour [9] and Kardomateas [10,11], Kardomateas and Phan [12], and Srinivas and Rao [13] used these solutions for the static buckling analysis of panels and plates; and Librescu et al. [14] used a stress function for a dynamic response. In general, these solutions are quite limited and they may exist only for specially prescribed boundary conditions. Hence, they serve as a benchmark only, rather than a general formulation/solution approach.

The layered approach has been implemented for sandwich panels by the first author and others through the high-order sandwich panel (HSAPT) approach, which assumes that the core is compliant and compressible with negligible in-plane rigidity. It has been extended recently by the authors to include stiff cores with in-plane rigidity, denoted as the extended HSAPT (EHSAPT). The HSAPT approach has been used extensively for static, dynamic, linear, and nonlinear applications for one-dimensional and two-dimensional problems: for example, free vibration (see work by Frostig and Baruch [15]); nonlinear behavior (see work by Sokolinsky and Frostig [16]); and free vibrations of plates (see work by Frostig and Thomsen [17]). In addition, the high-order model has been compared very well with finite element results and the elasticity solution; see work by Swanson and Kim [18] and, more recently, work by Santiuste et al. [19] for circular sandwich plates.

The enhanced approach (EHSAPT) should be used when the in-plane rigidity of the core cannot be neglected, such as solid medium to heavy weight foam or wood; or when local bending of the facesheets exists in cases such as wrinkling. It has recently been implemented for introduction of external in-plane loads through the core (see Frostig [20]) for wrinkling and global buckling of the sandwich pane (see Phan et al. [21]) and, recently, for free vibrations of sandwich panels (see Frostig et al. [22] and Phan et al. [23]).

The blast response has been also studied experimentally and theoretically: for example, Gardner et al. [24] experimentally investigated the blast response on sandwich narrow panels; and Dvorak et al. [25] investigated the response experimentally with comparisons with finite elements codes such as ABAQOUS or LS-Dyna. The underwater blast response of a circular sandwich panel at failure has also been investigated recently; see, for example, work by Latourte et al. [26]. Also, theoretical approaches have been considered for the blast response: for example, Hoo Fat and Palla [27] used a wave propagation approach in the in-plane and vertical directions to determine the response at failure of a clamped panel; Li et al. [28] used a fourth-order distribution through the thickness of the core along with a variational approach; and Mayercsik [29] used a finite element approach to determine the dynamic response.

The main goal of the paper is to present a computational model that is general, robust, and mathematically accurate yet simple that is able to determine the transient dynamic linear response of a sandwich panel when subjected to a blast type of loading where its shape is defined in time and space. The proposed model assumes that the behavior is elastic and linear with small displacements; the facesheets plates are assumed to possess in-plane and flexural rigidities with negligible shear rigidity and be loaded by the external loading schemes. In addition, the core is assumed to have shear stress and in-plane resistance, and its interfaces with the facesheets are fully bonded and can resist shear and vertical normal stresses. For validation, the dynamic EHSAPT model is compared with the closed-form elasticity solutions of a simply supported plate with a sinusoidal blast load.

The paper consists of a mathematical formulation that yields the equations of motion and the appropriate boundary conditions of the EHSAPT model. It is followed by a numerical study that compares the model results with those of elasticity, and it studies the response of a localized blast that is centered at midspan. Finally, a summary is presented and conclusions are drawn.

Mathematical Formulation

The mathematical formulation includes the derivation of the equations of motion along with the appropriate boundary conditions for the facesheets and core using Hamilton's principle that extremizes the Lagrangian, which consists of the kinetic energy and internal and external potential energies as follows:

$$\delta L = -\delta T + \int_{t_1}^{t_2} (\delta U + \delta V)\,\mathrm{d}t = 0 \tag{1}$$

where T is the kinetic energy; U and V are the strain energy and the potential of the external loads, respectively; t is the time coordinate between the times t_1 and t_2; and δ denotes the variational operator.

The first variation of the kinetic energy for the sandwich panel reads

$$\delta T = \sum_{j=t,b,c} \left(\int_{t_1}^{t_2} \int_{V_j} \rho_j u_{oj,t} \delta u_{oj,t} + \rho_j v_{oj,t} \delta v_{oj,t} + \rho_j w_{j,t} \delta w_{oj,t}\,\mathrm{d}V\,\mathrm{d}t \right) \tag{2}$$

where ρ_j $(j = t, b, c)$ is the density of the upper and lower facesheets and the core, respectively; $u_{j,t}$, $v_{j,t}$, and $w_{j,t}$ $(j = t, b, c)$ are the velocities in the longitudinal, transverse, and vertical directions or x, y, and z directions, respectively, of the various constituents of the panel; $f_{,t} = \partial f/\partial t$ is the first derivative of the function f with respect to the time coordinate; V_j $(j = t, b, c)$ is the volume of the upper and lower facesheets and core, respectively; and $\mathrm{d}V$ is the volume of a differential segment.

The first variation of the strain energy in terms of stresses and strains reads

$$\delta U = \sum_{j=t,b} \left(\int_{V_j} \delta\varepsilon_{xxj}\sigma_{xxj} + \delta\varepsilon_{yyj}\sigma_{yyj} + \delta\gamma_{xyj}\tau_{xyj}\,\mathrm{d}V \right) + \int_{V_c} \sigma_{xxc}\delta\varepsilon_{xxc} + \sigma_{yyc}\delta\varepsilon_{yyc} + \sigma_{zzc}\delta\varepsilon_{zzc} + \tau_{xyc}\delta\gamma_{xyc} + \tau_{xzc}\delta\gamma_{xzc} + \tau_{yzc}\delta\gamma_{yzc}\,\mathrm{d}V \tag{3}$$

where σ_{iij} and ε_{iij} $(i = x$ or y and $j = t, b, c)$ are the longitudinal and transverse (x and y) normal stresses and strains in the facesheets and core, respectively; τ_{xyj} and γ_{xyj} $(j = t, b, c)$ are the in-plane shear stress and shear angle, respectively, at the facesheets and core; τ_{izc} and γ_{izc} $(i = x$ or $y)$ are the vertical shear stresses and shear angle strain in the core on the longitudinal and transverse (x and y) faces of the core; x, y, and z denote the coordinates in the longitudinal, transverse, and vertical directions, respectively; and σ_{zzc} and ε_{zzc} are the (vertical) normal stresses and strains in the vertical direction of the core; see Fig. 1 for details.

The variation of the external work equals:

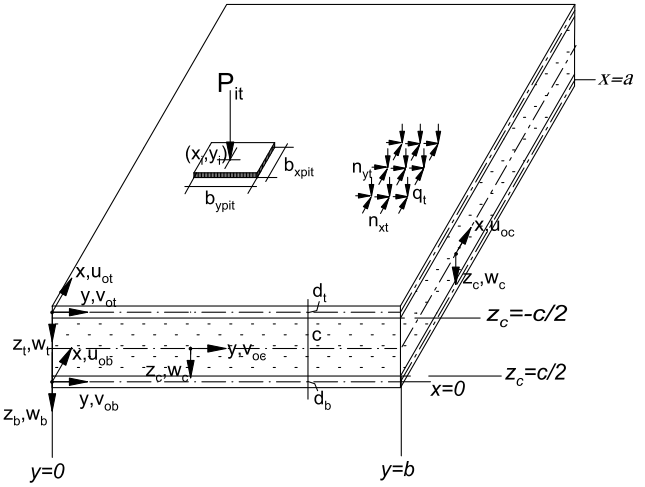

Fig. 1 Loading, coordinates system, and displacements of a typical sandwich plate.

Within the panel:

$$\delta V = -\sum_{j=t,b} \left(\int_0^b \int_0^a n_{xj}\delta u_{oj} + n_{yj}\delta v_{oj} + q_j \delta w_j\,\mathrm{d}x\,\mathrm{d}y \right) - \sum_{j=t,b} \left(\sum_{i=1}^{N_c} \left(\int_0^b \int_0^a \frac{P_{ij}\mathrm{Win}_{x,i}\mathrm{Win}_{y,i}\delta w_j}{b_{pxij}b_{pyij}}\,\mathrm{d}x\,\mathrm{d}y \right) \right)$$

where

$$\mathrm{Win}_{x,i} = H(x - x_i + 1/2b_{pxij}) - H(x - x_i - 1/2b_{pxij})$$
$$\mathrm{Win}_{y,i} = H(y - y_i + 1/2b_{pyij}) - H(y - y_i - 1/2b_{pyij}) \tag{4}$$

At the boundaries:

$$\delta V_{\mathrm{BC}} = -\sum_{xe=0,a} \alpha_{xbc} \sum_{j=t,b} \begin{pmatrix} \int_0^b N_{xxej}(x_e, y, t)\delta u_{oj}(x_e, y, t) + N_{xyej}(x_e, y, t)\delta v_{oj}(x_e, y, t) + \\ P_{xej}(x_e, y, t)\delta w_j(x_e, y, t) + M_{xxej}(x_e, y, t)\delta w_{j,x}(x_e, y, t) + \\ M_{xyej}(x_e, y, t)\delta w_{j,y}(x_e, y, t)\,\mathrm{d}y \end{pmatrix} - \sum_{ye=0,b} \alpha_{ybc} \sum_{j=t,b} \begin{pmatrix} \int_0^a N_{xyej}(x, y_e, t)\delta u_{oj}(x, y_e, t) + N_{yyej}(x, y_e, t)\delta v_{oj}(x, y_e, t) + \\ P_{yej}(x, y_e, t)\delta w_j(x, y_e, t) + M_{xyej}(x, y_e, t)\delta w_{j,x}(x, y_e, t) + \\ M_{yyej}(x, y_e, t)\delta w_{j,y}(x, y_e, t)\,\mathrm{d}x \end{pmatrix} \tag{5}$$

where $j = t, b$ refers to the upper and lower facesheets, respectively; u_{oj} and v_{oj}, are the in-plane-displacements in the longitudinal and transverse (x and y) directions at midheight of the facesheets; w_j are the vertical (z direction) displacements of the facesheets; n_{xj}, n_{yj}, and q_j $(j = t, b)$ are the external distributed loads in the coordinates directions, in-plane (x and y), and vertical loads, respectively, applied at the facesheets; P_{ij} are the vertical localized load resultants, centered at (x_i, y_i) and applied at the facesheets, and they are distributed on a b_{pxij} and b_{pxij} area (see Fig. 1); N_c is the number of concentrated loads, H is a Heaviside (ramp) function; N_{klej}, P_{kej}, and M_{klej} $(k = l = x, y)$ are external loads: in-plane, vertical, and bending moments applied at the edges of the panel; $w_{j,k}$ $(k = x$ and $y)$ is the slope of the vertical displacements; a and b are the length and width of the plate; $x_e = 0, a$ is the x coordinate of the edges, and similarly is $y_e = 0, b$; and α_{kbc} $(k = x, y)$ equals 1 when $x_e = a$ or $y_e = b$ and -1 when $x_e = 0$ or $y_e = 0$. See Fig. 1 for the geometry, sign convention for stresses, displacements, and loads.

The displacements of the facesheets follow the Navier assumption that the plane of section remains plane and perpendicular to the centroid plane after deformation, whereas the core displacements

take a general cubic and quadratic form as follows:

$$
\begin{aligned}
&u_j(x,y,z_j,t) = u_{oj} - w_{j,x}z_j, \qquad v_j(x,y,z_j,t) = v_{oj} - w_{j,y}z_j,\\
&\qquad w_j(x,y,z_j,t) = w_j \qquad (j=t,b)\\
&u_c(x,y,z_c,t) = u_o + \phi_x z_c + u_2 z_c^2 + u_3 z_c^3,\\
&\qquad v_c(x,y,z_c,t) = v_o + \phi_y z_c + v_2 z_c^2 + v_3 z_c^3,\\
&w_c(x,y,z_c,t) = w_o + w_1 z_c + w_2 z_c^2
\end{aligned} \tag{6}
$$

where z_j is the vertical coordinate of each facesheet measured downward from the centroid plane; u_k and v_k ($k = 0, 1, 2, 3$) are the unknown functions of the in-plane displacements of the core; ϕ_x and ϕ_y are its sections' slopes at its midheight; w_l ($l = 0, 1, 2$) are the vertical displacement unknowns, respectively; and z_c refers to the vertical coordinate of the core measured from its centroid downward. Please notice that all the unknown functions depend on x, y, and t only. Hence, the velocities of the facesheets and the core [see Eq. (2)] take the same shape.

The kinematic relations for the facesheets and the core assume small deformations and they read

$$
\begin{aligned}
&\varepsilon_{xxj} = -w_{j,xx}z_j + u_{oj,x}, \qquad \varepsilon_{yyj} = -w_{j,yy}z_j + v_{oj,y},\\
&\qquad \gamma_{xyj} = u_{oj,y} + v_{oj,x} - 2w_{j,xy} \qquad (j=t,b)\\
&\gamma_{xzc} = u_{c,z_c} + w_{c,x}, \qquad \gamma_{yzc} = v_{c,z_c} + w_{c,y}, \qquad \varepsilon_{zzc} = w_{c,z_c}
\end{aligned} \tag{7}
$$

The compatibility conditions at the upper and the lower face–core interfaces ($j = t, b$) in the longitudinal, transverse, and vertical (x, y, and z) directions are introduced into the mathematical formulation using six Lagrange multipliers through additional terms in the variation of the internal potential energy [see Eq. (3)] as follows:

$$
\delta U_{\text{comp}} = \delta\left[\int_0^a\int_0^b \begin{array}{l}(\lambda_{xt}(u_t(z_t = d_t/2) - u_c(z_c = -c/2)) +\\ \lambda_{yt}(v_t(z_t = d_t/2) - v_c(z_c = -c/2)) + \lambda_{zt}(w_t - w_c(z_c = -c/2) +\\ \lambda_{xb}(u_c(z_c = c/2) - u_b(z_b = -d_b/2))\\ +\lambda_{yb}(v_c(z_c = c/2) - v_b(z_b = -d_b/2)) + \lambda_{zb}(w_c(z_c = c/2) - w_b))\,\mathrm{d}x\,\mathrm{d}y\end{array}\right] \tag{8}
$$

where λ_{kj} ($k = x, y, z$ and $j = t, b$) are the Lagrange multiplier in each direction at the upper and lower face–core interfaces, respectively, that multiply the compatibility conditions at these interfaces that read

$$
\begin{aligned}
&-u_{ot} + u_o - 1/2u_1 c + 1/4u_2 c^2 - 1/8u_3 c^3 = 0\\
&-v_{ot} + v_o - 1/2v_1 c + 1/4v_2 c^2 - 1/8v_3 c^3 = 0\\
&-w_t + w_o - 1/2w_1 c + 1/4w_2 c^2 = 0\\
&u_{ob} - u_o - 1/2u_1 c - 1/4u_2 c^2 - 1/8u_3 c^3 = 0\\
&v_{ob} - v_o - 1/2v_1 c - 1/4v_2 c^2 - 1/8v_3 c^3 = 0\\
&w_b - w_o - 1/2w_1 c - 1/4w_2 c^2 = 0
\end{aligned} \tag{9}
$$

Please notice that each equation in Eq. (9) corresponds to the compatibility condition that multiplies each Lagrange multiplier in Eq. (8).

The equations of motion and the boundary conditions are derived using Eqs. (1) to (5) and the compatibility virtual work and compatibility conditions [Eqs. (8) and (9)] with the kinematic relations [Eq. (7)] and the distribution of the velocity of the facesheets and the core that correspond to the displacement distributions; see Eq. (6) and high-order stress resultants. Hence, after integration by parts and some algebraic manipulation, the equations of motion equations read:

Facesheets ($j = t, b$):

$$
\begin{aligned}
&M_j u_{oj,tt} - N_{xxj,x} - N_{xyj,y} + (-1)^k\lambda_{xj} - n_{xj} = 0\\
&M_j v_{oj,tt} - N_{xyj,x} - N_{yyj,y} + (-1)^k\lambda_{yj} - n_{yj} = 0\\
&-M_{yyj,yy} + M_j w_{j,tt} - M_{xxj,xx} + (-1)^k\lambda_{zj} - 1/2d_j\lambda_{xj,x} - 1/2d_j\lambda_{yj,y}\\
&-q_j - 2M_{xyj,xy} - I_{mj}w_{j,yytt} - I_{mj}w_{j,xxtt} = 0
\end{aligned} \tag{10}
$$

where $k = 1$ for $j = t$ and -1 for $j = b$, M_j ($j = t, b, c$), are the mass of facesheets and core, I_{mj} ($j = t, b$) are the rotary inertia of facesheets; and N_{klj} and M_{klj} ($k, l = x, y$ and $j = t, b, c$) are the in-plane and moment stress resultants of the normal and shear stress of the facesheets and core, respectively; see Fig. 2 for details.

Core:

$$
\begin{aligned}
&-N_{xxc,x} - \lambda_{xb} + M_c u_{o,tt} + \lambda_{xt} - N_{xyc,y} + \frac{1}{12}M_c c^2 u_{2,tt} = 0\\
&\frac{1}{12}M_c c^2 u_{1,tt} - M_{xxc,x} + \frac{1}{80}M_c c^4 u_{3,tt} - \frac{1}{2}c\lambda_{xb} - \frac{1}{2}c\lambda_{xt}\\
&- M_{xyc,y} + Q_{xc} = 0\\
&2M_{Q1xc} + \frac{1}{4}c^2\lambda_{xt} - \frac{1}{4}c^2\lambda_{xb} - M_{xy2c,y} + \frac{1}{80}M_c c^4 u_{2,tt}\\
&+ \frac{1}{12}c^2 M_c u_{o,tt} - M_{xx2c,x} = 0\\
&-\frac{1}{8}c^3\lambda_{xt} - \frac{1}{8}c^3\lambda_{xb} + \frac{1}{448}M_c c^6 u_{3,tt} + \frac{1}{80}M_c c^4 u_{1,tt}\\
&- M_{xy3c,y} - M_{xx3c,x} + 3M_{Q2xc} = 0\\
&\lambda_{yt} + \frac{1}{12}M_c c^2 v_{2,tt} - N_{xyc,x} - N_{yyc,y} + M_c v_{o,tt} - \lambda_{yb} = 0
\end{aligned}
$$

$$
\begin{aligned}
&-\frac{1}{2}c\lambda_{yt} - \frac{1}{2}c\lambda_{yb} - M_{xyc,x} - M_{yyc,y} + \frac{1}{80}M_c c^4 v_{3,tt}\\
&+ \frac{1}{12}M_c c^2 v_{1,tt} + Q_{yc} = 0\\
&- M_{xy2c,x} + 2M_{Q1yc} - M_{yy2c,y} + \frac{1}{80}M_c c^4 v_{2,tt} - \frac{1}{4}c^2\lambda_{yb}\\
&+ \frac{1}{12}M_c c^2 v_{o,tt} + \frac{1}{4}c^2\lambda_{yt} = 0\\
&-\frac{1}{8}c^3\lambda_{yt} - M_{yy3c,y} - M_{xy3c,x} + \frac{1}{80}M_c c^4 v_{1,tt} - \frac{1}{8}c^3\lambda_{yb}\\
&+ \frac{1}{448}M_c c^6 v_{3,tt} + 3M_{Q2yc} = 0\\
&\lambda_{zt} - Q_{xc,x} + \frac{1}{12}M_c c^2 w_{2,tt} - \lambda_{zb} - Q_{yc,y} + M_c w_{o,tt} = 0\\
&-M_{Q1yc,y} - \frac{1}{2}c\lambda_{zt} - \frac{1}{2}\lambda_{zb}c + \frac{1}{12}M_c c^2 w_{1,tt} - M_{Q1xc,x} + R_{zzc}\\
&= 0\\
&\frac{1}{12}M_c c^2 w_{o,tt} + \frac{1}{80}M_c c^4 w_{2,tt} - \frac{1}{4}\lambda_{zb}c^2 - M_{Q2yc,y}\\
&+ 2M_{zzc} + \frac{1}{4}c^2\lambda_{zt} - M_{Q2xc,x} = 0
\end{aligned} \tag{11}
$$

and the stress resultants in the facesheets and the core read

$$\{N_{klj}, M_{klj}\} = \int_{-(1/2)d_j}^{(1/2)d_j} (1, z_c)\sigma_{xxj}\,\mathrm{d}z_j \qquad (j = t, b)$$

$$\{N_{klc}, M_{klc}, M_{kl2c}, M_{kl3c}\} = \int_{-(1/2)c}^{(1/2)c} (1, z_c, z_c^2, z_c^3)\sigma_{xxc}\,\mathrm{d}z_c$$

$$\{Q_{kc}, M_{Q1kc}, M_{Q2kc}\} = \int_{-(1/2)c}^{(1/2)c} (1, z_c, z_c^2)\tau_{kzc}\,\mathrm{d}z_c,$$

$$\{R_{zzc}, M_{zzc}\} = \int_{-(1/2)c}^{(1/2)c} (1, z_c)\sigma_{zzc}\,\mathrm{d}z_c \tag{12}$$

where $k, l = x, y$; M_{kl2c} and M_{kl3c} are the high-order moments in the core due to in-plane normal stresses; Q_{kc} is the vertical shear stress resultant; M_{Qlkc} and M_{Q2kc} $(k = x, y)$ are the high-order moments due to vertical shear stresses in the core; and R_{zzc} and M_{zzc} are the stress resultant and the moments due to the vertical normal stresses. Notice that there are 23 equations of motion, where the first 17 are differential equations [see Eqs. (10) and (11)] and the last six, which are the compatibility conditions [see Eq. (9)] are algebraic. Please notice that a free traction edge, in the core, can be described only in the global sense, i.e., through null stress resultants rather than stresses. Or, in other words, the edge may not be free of stresses but its stress resultants at the edge are null.

The boundary conditions, at each edge of the panel, consist of 11 conditions and the corner conditions as follows:

At facesheets $(j = t, b)$:

At $x_e = 0(\alpha_{\mathrm{BC}} = -1)$,

$a(\alpha_{\mathrm{BC}} = 1)$:

$-N_{xxej} + \alpha_{\mathrm{BC}} N_{xxj} = 0 \quad \text{or} \quad u_{oj} - u_{oej} = 0$

$-N_{xyej} + \alpha_{\mathrm{BC}} N_{xyj} = 0 \quad \text{or} \quad v_{oj} - v_{oej} = 0$

$-M_{xxej} - \alpha_{\mathrm{BC}} M_{xxj} = 0 \quad \text{or} \quad w_{j,x} - w_{je,x} = 0$

$-P_{xej} + \alpha_{\mathrm{BC}}(2M_{xyj,y} + M_{xxj,x} + 1/2d_j\lambda_{xj} + I_{mj}w_{j,xtt}) = 0$ or $w_j - w_{je} = 0$

At $y_e = 0(\alpha_{\mathrm{BC}} = -1)$,

$b(\alpha_{\mathrm{BC}} = 1)$:

$-N_{xyej} + \alpha_{\mathrm{BC}} N_{xyj} = 0 \quad \text{or} \quad u_{oj} - u_{oej} = 0$

$-N_{yyej} + \alpha_{\mathrm{BC}} N_{yyj} = 0 \quad \text{or} \quad v_{oj} - v_{oej} = 0$

$-M_{yyej} - \alpha_{\mathrm{BC}} M_{yyj} = 0 \quad w_{j,y} - w_{je,y} = 0$

$-P_{yej} + \alpha_{\mathrm{BC}}(2M_{xyj,x} + M_{yyj,y} + 1/2d_j\lambda_{yj} + I_{mj}w_{j,ytt}) = 0$ or $w_j - w_{je} = 0$

At $x_e = 0, a$, and $y_e = 0, b$:

$-2M_{xyj} = 0 \quad \text{or} \quad w_j = 0$ (13)

At core:

At $x_e = 0, \quad a$:

$N_{xxc} = 0$ or $u_o - u_{oe} = 0$, $\quad M_{xxc} = 0$ or $\phi_x - \phi_{xe} = 0$,

$M_{xx2c} = 0$ or $u_2 - u_{2e} = 0$, $\quad M_{xx3c} = 0$ or $u_3 - u_{3e} = 0$,

$N_{xyc} = 0$ or $v_o - v_{oe} = 0$, $\quad M_{xyc} = 0$ or $\phi_y - \phi_{ye} = 0$,

$M_{xy2c} = 0$ or $v_2 - v_{2e} = 0$, $\quad M_{xy3c} = 0$ or $v_3 - v_{3e} = 0$,

$Q_{xc} = 0$ or $w_o - w_{oe} = 0$, $\quad M_{Q1xc} = 0$ or $w_1 - w_{1e} = 0$,

$M_{Q2xc} = 0$ or $w_2 - w_{2e} = 0$

At $y_e = 0, b$:

$N_{xyc} = 0$ or $u_o - u_{oe} = 0$, $\quad M_{xyc} = 0$ or $\phi_x - \phi_{xe} = 0$

$M_{xy2c} = 0$ or $u_2 - u_{2e} = 0$, $\quad M_{xy3c} = 0$ or $u_3 - u_{3e} = 0$,

$N_{yyc} = 0$ or $v_o - v_{oe} = 0$, $\quad M_{yyc} = 0$ or $\phi_y - \phi_{ye} = 0$,

$M_{yy2c} = 0$ or $v_2 - v_{2e} = 0$, $\quad M_{yy3c} = 0$ or $v_3 - v_{3e} = 0$

$Q_{yc} = 0$ or $w_o - w_{oe} = 0$, $\quad M_{Q1yc} = 0$ or $w_1 - w_{1e} = 0$

$M_{Q2yc} = 0$ or $w_2 - w_{2e} = 0$ (14)

Please notice that the force boundary conditions in the core do not require corner conditions.

To define the governing equations of motion, the constitutive relations for the various constituents must be defined first. The relations for the isotropic facesheet are those of an ordinary plate following Eq. (12), and they read $(j = t, b)$

$$N_{xxj} = A_j(\mu_j v_{oj,y} + u_{oj,x}), \qquad N_{yyj} = A_j(\mu_j u_{oj,x} + v_{oj,y}),$$
$$N_{xxj} = 1/2A_j(1 - \mu_j)(u_{oj,y} + v_{oj,x})$$
$$M_{xxj} = -D_j(\mu_j w_{j,yy} + w_{j,xx}), \qquad M_{yyj} = -D_j(\mu_j w_{j,xx} + w_{j,yy}),$$
$$M_{xxj} = -D_j(1 - \mu_j)w_{j,xy} \tag{15}$$

where

$$A_j = \frac{E_j d_j}{-\mu_j^2 + 1}, \qquad D_j = 1/12\frac{E_j d_j}{-\mu_j^2 + 1} \qquad (j = t, b)$$

are the in-plane and flexural rigidities of the various facesheets, respectively; E_j is the modulus of elasticity of the facesheets; and μ_j is the Poisson ratio.

The relations for the core are those of a three-dimensional isotropic elastic medium, and they read

$$\sigma_{xxc} = \frac{E_c((\varepsilon_{xxc} - \varepsilon_{yyc} - \varepsilon_{zzc})\mu_c - \varepsilon_{xxc})}{2\mu_c^2 + \mu_c - 1},$$
$$\sigma_{yyc} = -\frac{E_c((\varepsilon_{xxc} - \varepsilon_{yyc} + \varepsilon_{zzc})\mu_c + \varepsilon_{yyc})}{2\mu_c^2 + \mu_c - 1},$$
$$\sigma_{zzc} = -\frac{E_c((\varepsilon_{xxc} + \varepsilon_{yyc} - \varepsilon_{zzc})\mu_c + \varepsilon_{zzc})}{2\mu_c^2 + \mu_c - 1},$$
$$\tau_{xyc} = G_{xyc}\gamma_{xyc}, \qquad \tau_{xzc} = G_{xzc}\gamma_{xzc}, \qquad \tau_{yzc} = G_{yzc}\gamma_{yzc} \tag{16}$$

where E_c is the modulus of elasticity of the core, G_{xyc} is the in-plane shear modulus, G_{kz} $(k = x$ or $y)$ is the vertical shear modulus, and the strains are defined in Eq. (7). Hence, the stress resultants displacements following Eq. (12) read

$$N_{xxc} = \frac{E_c(((u_{2,x} - v_{2,y})c^2 - 12w_1 + 12u_{o,x} - 12v_{o,y})\mu_c - c^2u_{2,x} - 12u_{o,x})c}{12(2\mu_c^2 + \mu_c - 1)}$$

$$M_{xxc} = -3\left(\left(-\frac{20}{3}\mu_c + \frac{20}{3}\right)\phi_{x,x} - c^2(\mu_c - 1)u_{3,x} + \mu_c\left(c^2v_{3,y} + \frac{20}{3}\phi_{y,y} + \frac{40}{3}w_2\right)\right)$$

$$E_c c^3(240(2\mu_c^2 + \mu_c - 1))^{-1}$$

$$M_{xx2c} = -3\left(-c^2(\mu_c - 1)u_{2,x} + \left(-\frac{20}{3}\mu_c + \frac{20}{3}\right)u_{o,x} + \left(c^2v_{2,y} + \frac{20}{3}v_{o,y} + \frac{20}{3}w_1\right)\mu_c\right)$$

$$E_c c^3(240(2\mu_c^2 + \mu_c - 1))^{-1}$$

$$M_{xx3c} = -5\left(\left(-\frac{28}{5}\mu_c + \frac{28}{5}\right)\phi_{x,x} - c^2(\mu_c - 1)u_{3,x} + \mu_c\left(c^2v_{3,y} + \frac{28}{5}\phi_{y,y} + \frac{56}{5}w_2\right)\right)$$

$$E_c c^5(2240(2\mu_c^2 + \mu_c - 1))^{-1}$$

$$N_{yyc} = \frac{(c^2(\mu_c - 1)v_{2,y} + (12\mu_c - 12)v_{o,y} - \mu_c(c^2u_{2,x} + 12u_{o,x} + 12w_1))E_c c}{12(2\mu_c^2 + \mu_c - 1)}$$

$$M_{yyc} = 3\left(\left(\frac{20}{3}\mu_c - \frac{20}{3}\right)\phi_{y,y} + c^2(\mu_c - 1)v_{3,y} - \mu_c\left(u_{3,x}c^2 + \frac{40}{3}w_2 + \frac{20}{3}\phi_{x,x}\right)\right)$$

$$E_c c^3(240(2\mu_c^2 + \mu_c - 1))^{-1}$$

$$M_{yy2c} = 3\left(c^2(\mu_c - 1)v_{2,y} + \left(\frac{20}{3}\mu_c - \frac{20}{3}\right)v_{o,y} - \left(c^2u_{2,x} + \frac{20}{3}w_1 + \frac{20}{3}u_{o,x}\right)\mu_c\right)$$

$$E_c c^3(240(2\mu_c^2 + \mu_c - 1))^{-1}$$

$$M_{yy3c} = 5\left(\left(\frac{28}{5}\mu_c - \frac{28}{5}\right)\phi_{y,y} + c^2(\mu_c - 1)v_{3,y} - \left(u_{3,x}c^2 + \frac{56}{5}w_2 + \frac{28}{5}\phi_{x,x}\right)\mu_c\right)$$

$$E_c c^5(2240(2\mu_c^2 + \mu_c - 1))^{-1}$$

$$N_{xyc} = \frac{1}{12}G_{xyc}(u_{2,y} + v_{2,x})c^3 + G_{xyc}(u_{o,y} + v_{o,x})c,$$

$$M_{xyc} = \frac{1}{240}G_{xyc}c^3(3c^2u_{3,y} + 3c^2v_{3,x} + 20\phi_{x,y} + 20v_{1,x})$$

$$M_{xy2c} = \frac{1}{240}G_{xyc}c^3(3c^2u_{2,y} + 3c^2v_{2,x} + 20u_{o,y} + 20v_{o,x}),$$

$$M_{xy3c} = \frac{1}{2240}G_{xyc}c^5(5c^2u_{3,y} + 5c^2v_{3,x} + 28\phi_{x,y} + 28\phi_{y,x})$$

$$Q_{xzc} = \frac{1}{4}\left(c^2u_3 + \frac{1}{3}c^2w_{2,x} + 4\phi_x + 4w_{o,x}\right)G_{xzc}c, \qquad M_{Q1xc} = \frac{1}{12}G_{xzc}(2u_2 + w_{1,x})c^3$$

$$M_{Q2xc} = \frac{1}{240}G_{xzc}c^3(9c^2u_3 + 3c^2w_{2,x} + 20\phi_x + 20w_{o,x})$$

$$Q_{yc} = \frac{1}{4}\left(c^2v_3 + \frac{1}{3}c^2w_{2,y} + 4\phi_y + 4w_{o,y}\right)G_{yzc}c, \qquad M_{Q1yc} = \frac{1}{12}G_{yzc}(2v_2 + w_{1,y})c^3$$

$$M_{Q2yc} = \frac{1}{240}G_{yzc}c^3(9c^2v_3 + 3c^2w_{2,y} + 20\phi_y + 20w_{o,y})$$

$$R_{zzc} = -\frac{((-12\mu_c + 12)w_1 + \mu_c(c^2u_{2,x} + c^2v_{2,y} + 12u_{o,x} + 12v_{o,y}))E_c c}{12(2\mu_c^2 + \mu_c - 1)}$$

$$M_{zzc} = -3\left(\left(-\frac{40}{3}\mu_c + \frac{40}{3}\right)w_2 + \mu_c\left(c^2v_{3,y} + u_{3,x}c^2 + \frac{20}{3}\phi_{y,y} + \frac{20}{3}\phi_{x,x}\right)\right)$$

$$E_c c^3(240(2\mu_c^2 + \mu_c - 1))^{-1} \tag{17}$$

A similar approach, which is not presented for brevity, may be used for the case of an orthotropic core.

The equations of motion consist of the following 23 unknowns: the in-plane displacements of the midplane, in x and y directions; the vertical displacements of the upper and the lower facesheets; the six Lagrange multipliers; and the 11 polynomial coefficients of the core [see Eq. (6)]. The first six governing equations are determined by substitution of the constitutive relations [see Eq. (15)] in Eq. (10), and the next 11 equations are derived by substitution of the stress resultants of the core [see Eq. (17)] into Eq. (11). The additional six compatibility conditions remain unchanged. For brevity, the governing equations are not presented. This set of equations consists of initial value, ordinary differential and algebraic equations, denoted as differential-algebraic equations (DAEs). Two methods of solution have been considered: the first one isolates the unknown functions from the algebraic equations and inserts the results into the remaining ordinary differential equations (ODEs), thus yielding a lower number of equations that are all ODEs but more complicated. The second method numerically solves the set of the DAEs using a special Maple solver (see Char et al. [30]) for DAEs, and it proved here to be more efficient than the first one.

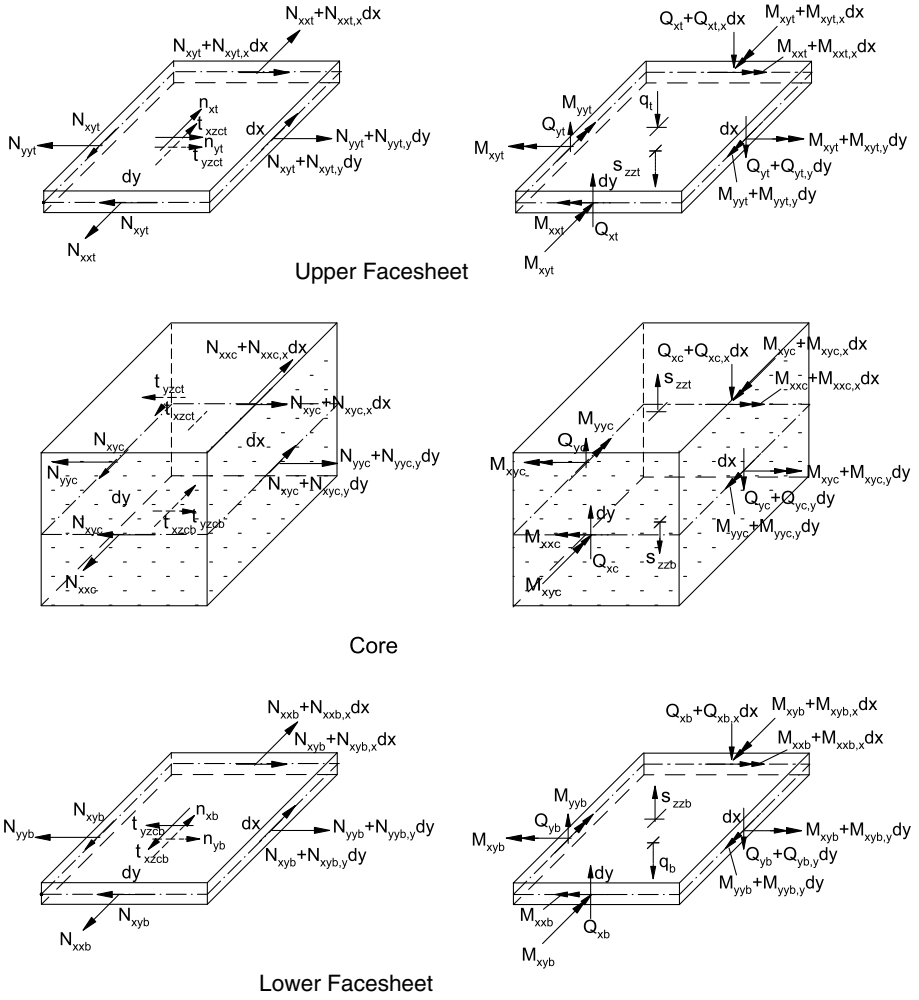

Fig. 2 In-plane stress resultants, bending moments, and shear resultants of differential elements of the various constituents of the plates.

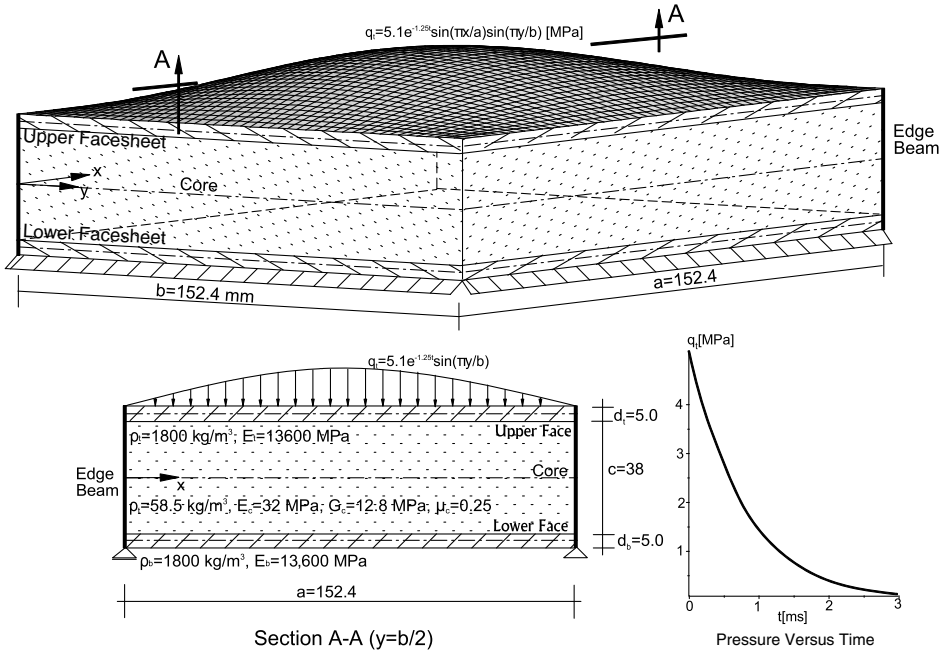

Fig. 3 Geometry and mechanical properties of a specific sandwich panel and the loading scheme of a fully distributed sinus blast pressure and its time function.

Numerical Study

The numerical study presents the blast response of a simply supported, square sandwich plate when subjected to a fully and localized distributed blast load. The boundary conditions of the plate assume that the upper and the lower facesheets are simply supported and that the vertical displacements of the edges of the core are prevented. These conditions are fulfilled through the use of a special edge beam; see Fig. 3 for details. The panel considered is based on a specific setup used in an experimental blast investigation of Gardner et al. [24], with some modifications. In both cases, the results include deformed shapes between 0.05 and 1 ms every 0.1 ms, displacements, stresses at interfaces and within the depth of the core, and stress resultants of the facesheets and core. In the first case, a comparison with the elasticity solution (see work by Kardomateas et al. [31]) is presented.

The square panel, $a = b = 152.4$ mm, consists of two facesheets and a core. The facesheets are made of E-glass vinyl-ester laminated composite with a quasi-isotropic layup, $[0/45/90/-45]_s$. It has a density of 1800 kg/m^3, an equivalent modulus of elasticity of 13,600 MPa, and a foam core. The core (A300) is a Corecell™ A-series styrene acrylonitrile foam with a density of 58.5 kg/m^3, an elasticity modulus of 32 MPa, a Poisson ratio of 0.25, and a shear modulus of 12.8 MPa. In the case of the full blast case, the core properties are different; see next.

Blast Pressure: Fully Distributed

The first case consists of a fully distributed sinusoidal pressure load applied at the upper facesheets only and equals $q_t = 5.1e^{-1.25t} \sin(\pi x/a) \sin(\pi y/b)$ MPa, where a and b are the length and width of the plates, respectively; and t is measured in milliseconds. For the geometry, mechanical properties, and pressure distribution in space and time, see Fig. 3. Please notice that the blast load almost diminishes after 3 ms. This case is used for comparison with the benchmark of the elasticity solution by Kardomateas et al. [31]. It includes the deformed shapes at the first millisecond in Fig. 4; the values of the displacements versus time at the facesheets and the core in Fig. 5; and the interfacial stresses at the face–core interfaces versus time in Fig. 6. Here, the data of the elasticity solution consisted of the data of the facesheets described in the previous paragraph and the following data for the core: $E_c = 32.0$ MPa, $G_c = 20.0$ MPa, and the Poisson ratio of $\mu_{xy} =$

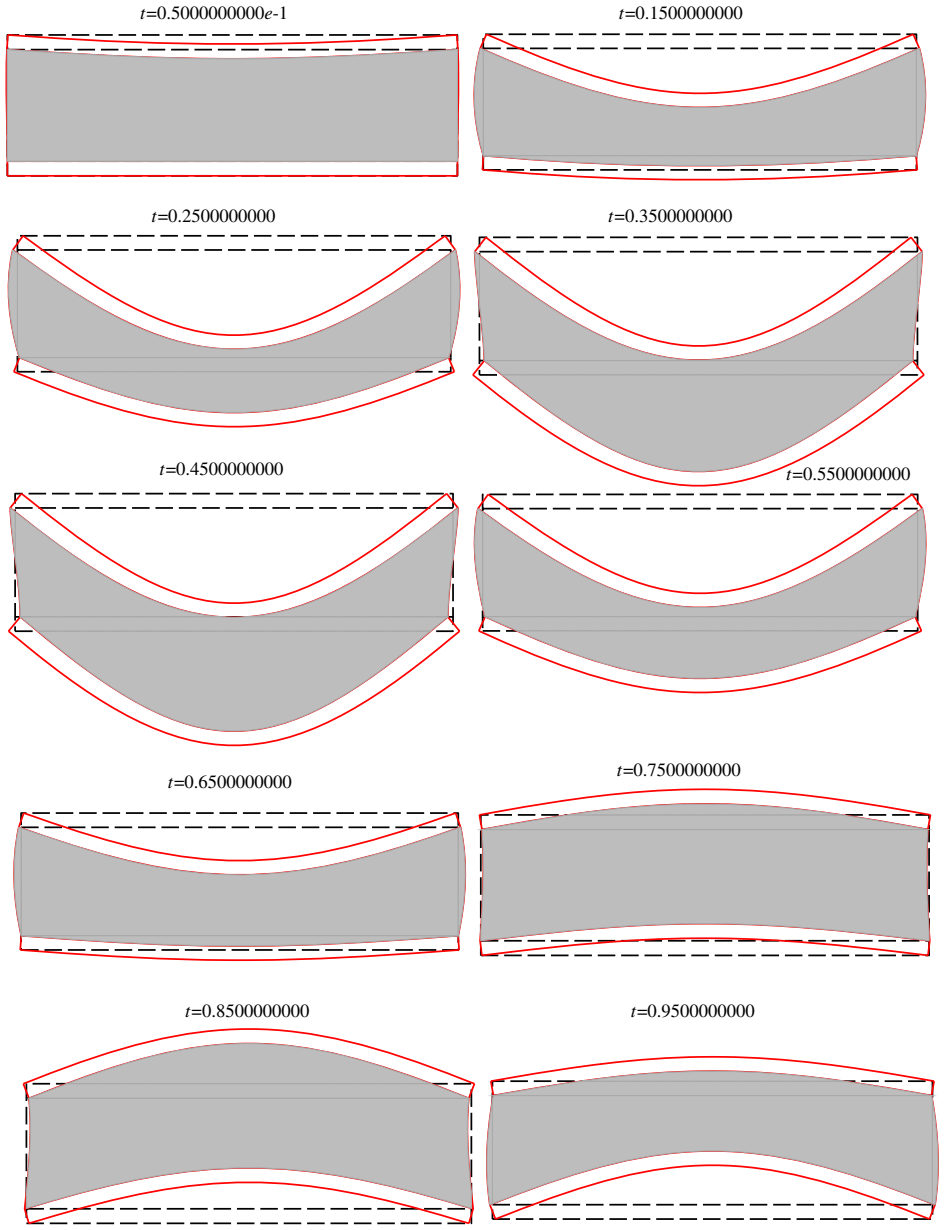

Fig. 4 Deformed shapes, in the first millisecond, at section A-A (Fig. 3) of a panel loaded with a fully sinusoidal distributed blast load applied at its upper facesheet.

0.25 and $\mu_{xz} = \mu_{yz} = 0.35$ for the facesheets and the core. The data used here in the EHSAPT model include the same data as that of the elasticity but with $\mu_{xy} = \mu_{xz} = \mu_{yz} = 0.25$ for the facesheets and $\mu_{cxy} = 0.25$ and $\mu_{cxz} = \mu_{cyz} = 0.35$ for the core.

The deformed shape of the section A-A (Fig. 3) that passes through center of panel, at $y = b/2$, appears in Fig. 4. It demonstrates qualitatively, but based on accurate numerical results, how the overall response of the panel evolves with time at the first millisecond and clarifies the wave propagation that occurs between the two facesheets longitudinally as well as vertically. Initially, the upper loaded facesheets move vertically, whereas the lower facesheet is still at rest. It is followed by large deformation of the upper facesheets but with a small deformation in the lower facesheets, thus leading to a significant reduction of the thickness of the core. In the next time step, $t = 0.25$ ms, the deformations of the lower facesheet increase, whereas those of the upper one do not change significantly. In the next time steps, both facesheets almost move together with a small extension in the core thickness. The response starts to change direction at $t = 0.55$. Here, the lower facesheet moves upward but not in tandem with the upper facesheet that still has significant vertical displacements; see $t = 0.65$ ms. Above that time step, the two facesheets move upward with unequal displacements. Please notice that, during that time, the core height is changing from contraction to expansion and the shape of its edge section changes from expansion to an S-type shape and to contraction. All these patterns are results of the waves that travel along the panel and through the core, in the vertical direction, between the two facesheets.

The vertical displacement at midspan and the in-plane displacements at the center of the support line at the x and y edges of the facesheets and at the midheight of the core versus time appear in Fig. 5. A very good correlation with the elasticity solution is observed. The displacements almost coincide at the first 1.5 ms, and the differences enlarge toward the end of the duration. These differences are due to the numerical damping that occurs in the numerical inverse Laplace used for the elasticity solution; see Kardomateas et al. [31]. It is similar to the damping that occurs when time difference methods such as the Newmark method or others are used. Please notice that the EHSAPT is solved using the initial value DAE solvers of Maple [30] with an absolute and relative error of 10^{-7}. The vertical displacements at midspan in Fig. 5a reveal that the displacements of the lower facesheets are larger at the initiation (about 0.25 ms) of the blast as compared with the loaded facesheets; see the deformed shape at $t = 0.25$ ms for clarification. It occurs as a result of the incident wave that travels from the loaded facesheets to the lower facesheet through the core. The vertical displacement of the core corresponds to an average of the displacements of the facesheets. In addition, notice that

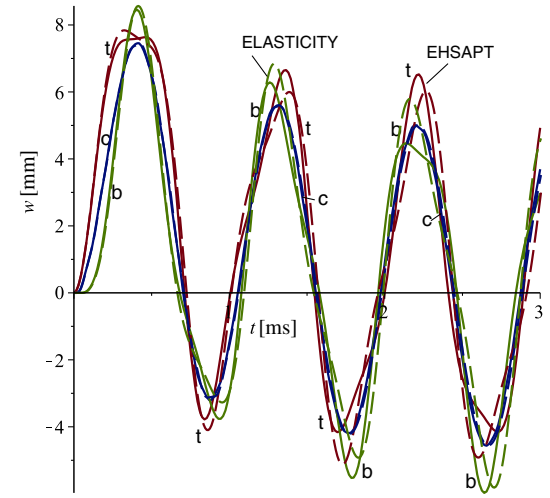

a) Vertical displacements at center of plate

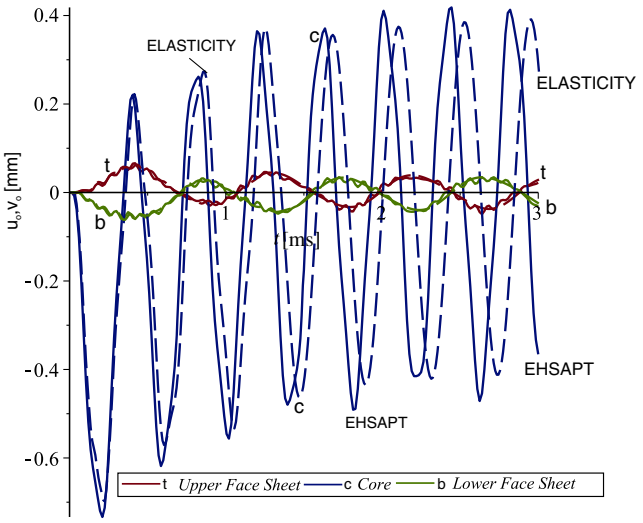

b) In-Plane displacements, x and y dir., at center of support line

Fig. 5 Displacements versus time of the facesheets and core for a fully distributed blast loading with comparison to the elasticity solution (Kardomateas et al. [31]) (solid line = EHSAPT, dashed line = elasticity).

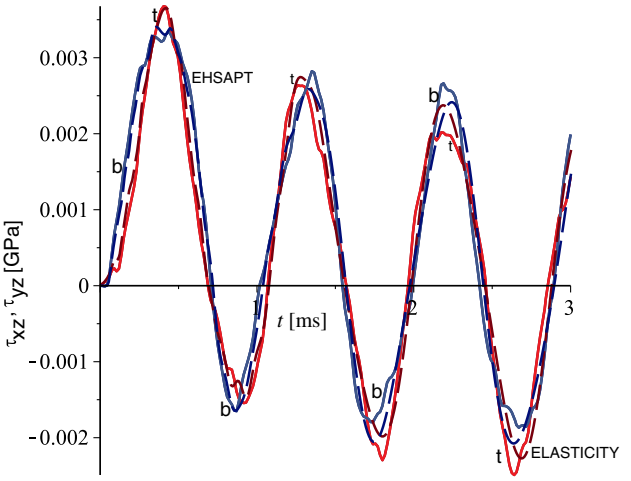

a) Shear stresses at center of edge support

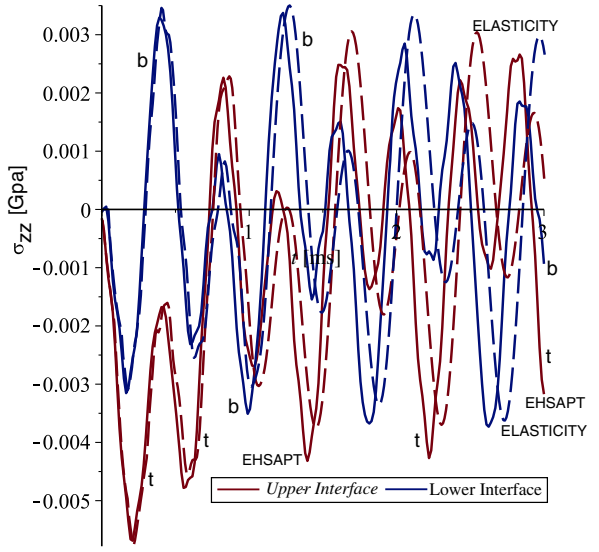

b) Vertical normal stresses at center of plate

Fig. 6 Interfacial stresses versus time at face–core interfaces due to fully distributed blast loading with comparison to elasticity (Kardomateas et al. [31]) (solid line = EHSAPT, dashed line = elasticity).

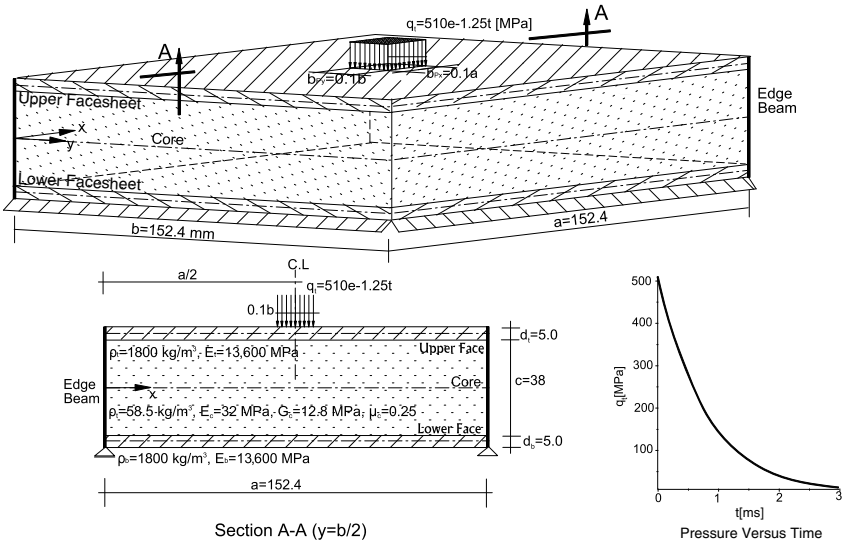

Fig. 7 Geometry and mechanical properties of a specific panel loaded by localized blast distribution centered in the midst of the plate along with a measured time function (C.L., center line).

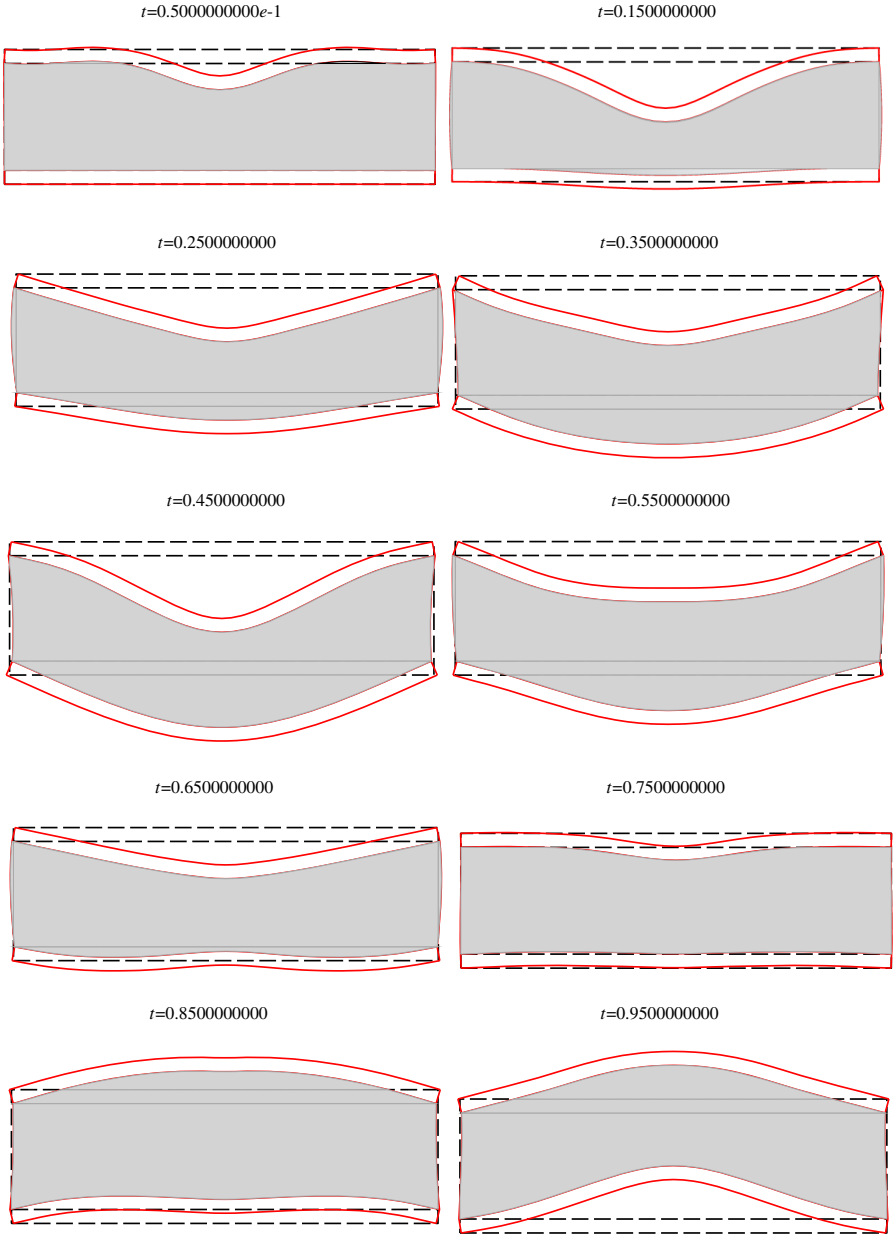

Fig. 8 Deformed shapes, in the first millisecond, at section A-A (Fig. 7) of a localized uniformly distributed blast load applied at the upper facesheet.

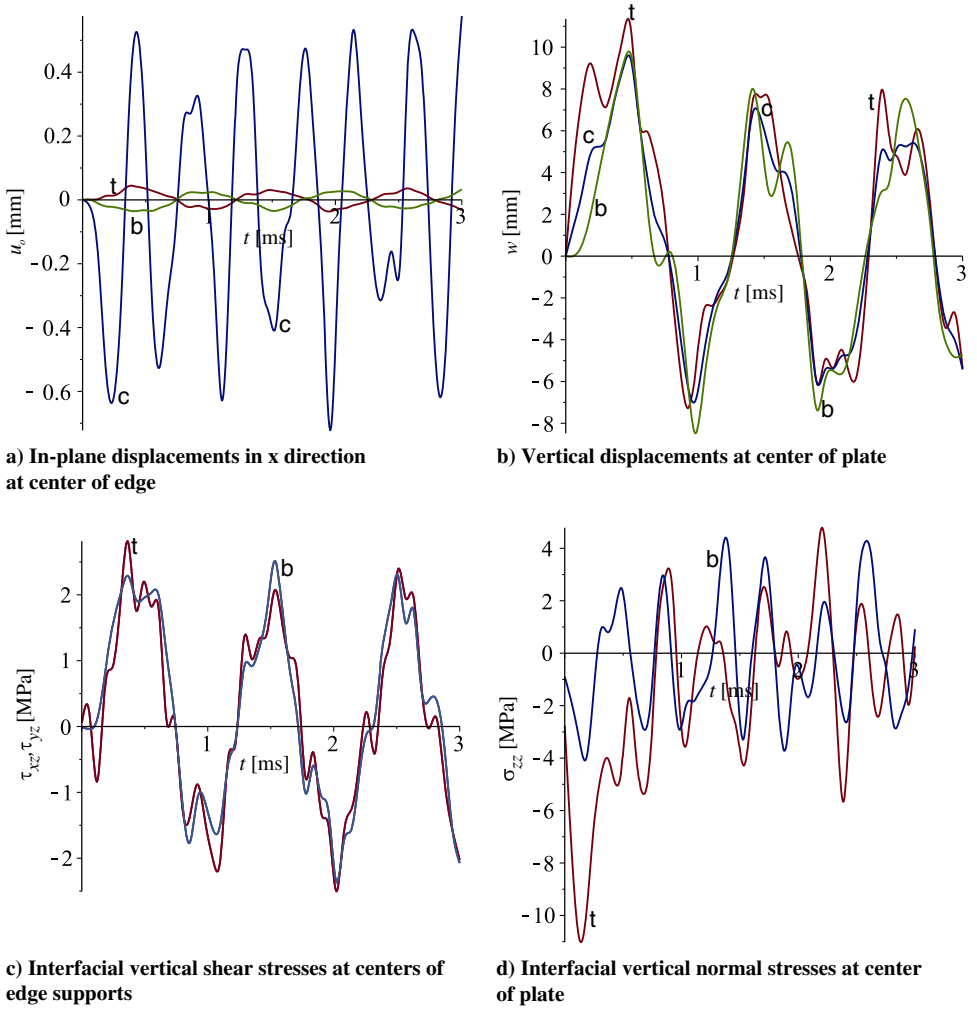

a) In-plane displacements in x direction at center of edge

b) Vertical displacements at center of plate

c) Interfacial vertical shear stresses at centers of edge supports

d) Interfacial vertical normal stresses at center of plate

Fig. 9 Displacements of facesheets and core and interfacial stresses versus time of a distributed localized blast load (solid line = EHSAPT, dashed line = elasticity).

the period of the transient response is about 1.7 ms. The in-plane displacements of the facesheets and the midheight of the core in the x and y directions are identical; see Fig. 5b. Here, the in-plane displacements of the facesheets coincide with the elasticity solution, and they are quite small as compared with those of the midheight of the core. The discrepancy between the EHSAPT and the elasticity increases with time due to the numerical damping phenomenon involved in the elasticity solution. In addition, the magnitudes of these displacements, at the midheight of the core, are much larger than those of the facesheets; and its time period is much smaller than that of the facesheets.

The interfacial stresses versus time at the face–core interfaces at the center of the plate and the center of support line in the x and y directions appear in Fig. 6. A very good correlation with the elasticity benchmark is observed. The interfacial shear stresses, at the center of the support lines in the EHSAPT and the elasticity solution (see Fig. 6a), almost coincide through the first 3 ms with a time period of about 1.3 ms. Here, the interfacial shear stresses at the upper and the lower interfaces are in tandem, and they are almost identical except for extreme values. The vertical normal stresses at the interfaces appear in Fig. 6b, and they reveal almost an erratic response, with very short time periods much smaller than those of the adjacent shear stresses. The comparison is very satisfactory at the first milliseconds, and the differences enlarge with time due to the numerical damping involved with the elasticity solution. Notice that the interfacial normal stresses, at the upper and lower face–core interfaces, are in tandem; and their extreme values are reached at the same time but with different values.

In general, a very satisfactory comparison between the elasticity and the EHSAPT model is detected, especially at the first 1.5 ms.

Blast Pressure: Locally Distributed

This case investigates the blast response of a localized pressure load, located in the vicinity of center of the plate and uniformly distributed at the upper facesheet, on a square area of $0.1a \times 0.1b$ with a blast pressure of $510e^{-1.25t}$ MPa; see Fig. 7 for details. The transient dynamic response here has been solved using a Fourier series description of the localized pressure with nine terms in each direction, which proved to converge. The results are described in terms of deformed shapes at the first millisecond at various time steps in addition to displacements, stress resultants of the facesheets and core, interfacial shear and vertical normal stresses versus time, and for a specific time at $y = b/2$ versus x, as well as distributions of the displacements and stresses of the core through its depth at different times.

The deformed shapes of section A-A (Fig. 7) that passes through center of the plate, at $y = b/2$, at various time steps in the first millisecond appear in Fig. 8. At the initial time steps ($t = 0.05$ to 0.95 ms), the localized load is associated with significant vertical displacements around the center of the plate, with almost no movement of the lower facesheet. Hence, the initial response is localized and is concentrated in the vicinity of the localized load, which is similar to a localized load on an elastic foundation. However, in the next time step ($t = 0.25$ to 0.35 ms), the panel starts to behave as a sandwich plate where the two facesheets are moving downward but with unsmooth displacement patterns due to the localized loads

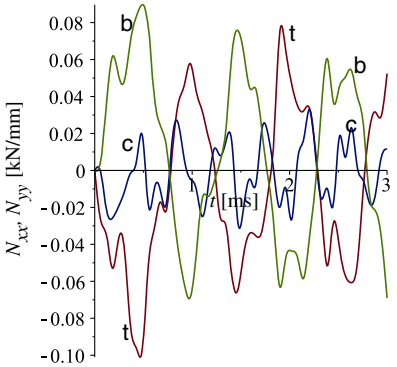

a) In-plane normal stress resultants at center of edge support

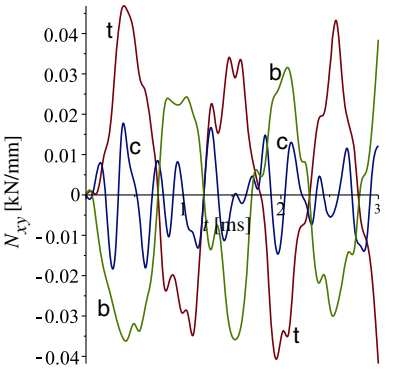

b) In-plane shear stress resultants at corners of plate

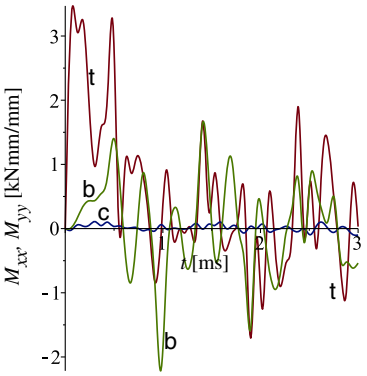

c) Bending moments stress resultants at center of plate

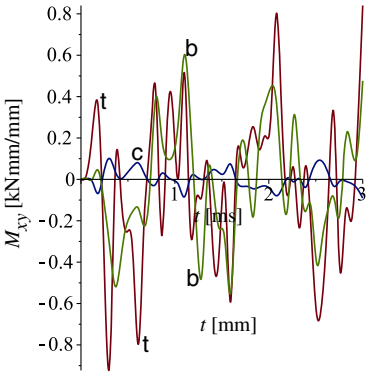

d) Twisting moments in face sheets and core at corners of plate

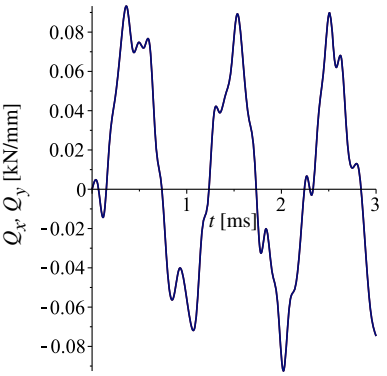

e) Vertical shear stress resultants in core at center of support edge

Fig. 10 Stress resultants in facesheets and core versus time of a localized distributed blast load; top-red(t), bot-blue(b), core-green(c).

(see deformed shape at $t = 0.35$ ms), and it is intensified at $t = 0.45$ ms. The deformations change directions at $t = 0.55$ ms and above, where the lower facesheets move upward, whereas the upper loaded facesheets are still downward. It almost returns to the response at the first time step at $t = 0.75$ ms, and both of them move upward above $t = 0.85$ ms. These shapes reveal that, in the first millisecond, the traveling waves are a mixture of in-plane and flexural waves in the facesheets, as well as in the vertical ones through the depth of the core. Please notice that, due to the large displacements, the magnification factors of the drawing of the displacements here are half of that of the previous case.

The displacements and the interfacial stresses versus time appear in Fig. 9. The in-plane displacements, in x and y directions, at the midheight of the facesheets and the core at the center of the supports appear in Fig. 9a. In general, the displacements are of the same order as for the first case with the fully distributed pressure but with a pressure load resultant that is almost one-quarter of that of first case. It also reveals a very fast fluctuation for the core and a much slower fluctuation for the facesheets. Here, the displacements of the core are almost an order larger than those of the facesheets. Notice that the trends here are similar to those of the fully distributed blast; see Fig. 5b. The vertical displacements at the center of the plate (see Fig. 9b) and are of an order larger than the in-plane ones but with much larger time periods similar to those of the first case (see Fig. 5a). Here, the curves are with local fluctuation, although the extreme values are of similar order and at the same times as compared with the previous case. Similar trends, but with local fluctuation as compared with the fully distributed case (see Fig. 6), occur for the shear interfacial stresses at the panel supports (see Fig. 9c) and the vertical normal interfacial stresses at the center of the plate (see Fig. 9d). Also, here, the time periods of the vertical normal stresses are much smaller than those of the shear stresses.

The stress resultants of the facesheets and the core versus time appear in Fig. 10, and they all reveal large fluctuations with short and long time periods. Notice that the in-plane resultants, at the center of the plate, in the x and y directions are identical; and the contribution of the core is small as compared with those of the facesheets (see Fig. 10a). Similar observations are detected for the in-plane shear stress resultants, at the supports of the plate, but smaller in values as compared with the in-plane normal stress resultants (see Fig. 10b). The bending moments in the x and y directions at the center of the plate are identical (see Fig. 10c) and with a very small contribution of the core. Similar trends are observed for the torsion moments at the corners of the plate (see Fig. 10d) but with values that are an order smaller than those of the bending moments. Finally, in Fig. 10e, the vertical shear stress resultants, at the supports of the plate, of the core are presented. They are similar to those of the interfacial shear stresses (see Fig. 9c), since the distribution of the shear stresses through the depth of the core is almost uniform (see Fig. 11f).

The distributions of the displacements and stresses at various time steps, at the center of the support line and the plate through the depth of the core, appear in Fig. 11. The in-plane displacements, in the x and y directions, at the center of the supports (see Fig. 11a), take a cubic shape at the various times and changes from negative to positive values, whereas the vertical displacements, at the center of the plate, are quadratic but with a small curvature (see Fig. 11b) and large changes, between the upper and the lower displacements of the core interfaces at the initiation of the blast. The in-plane normal stresses, in the x and y directions at the center of the plate, are cubic and at low time steps are in tension and compression with identical signs through depth of core, see Fig. 11c, and they take different signs at the $t = 3.0$ ms. Hence, the contribution of the core to the overall bending is quite small at the beginning of

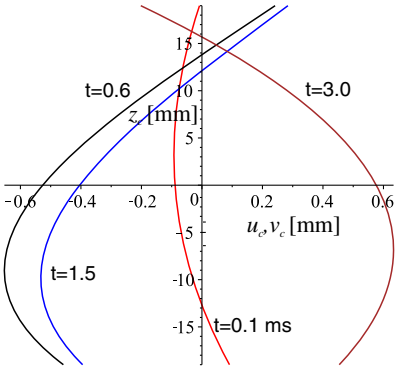

a) In-plane (x and y dir.) at center of edge supports

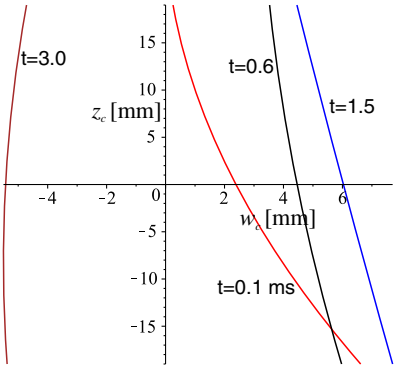

b) Vertical displacements at center of plate

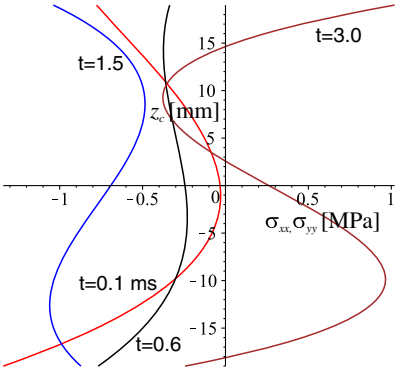

c) In-plane normal stresses at center of plate

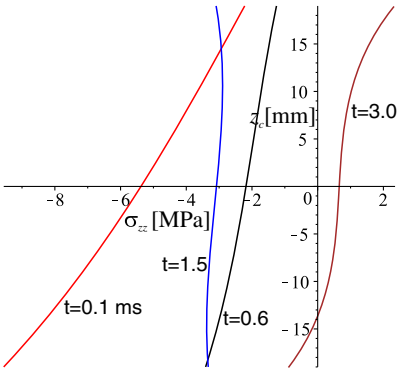

d) Vertical normal stresses at center of plate

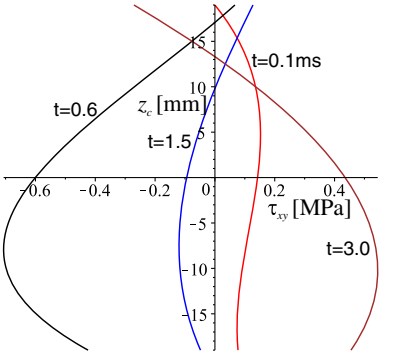

e) In-plane shear stresses at corners of plate

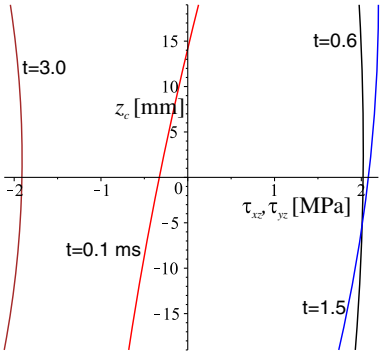

f) Vertical shear stresses at center of edge supports

Fig. 11 Displacements and stress distribution versus time through depth of core of a localized distributed blast load.

the blast and it increases with time. The vertical normal stresses at the plate center are almost linear or very close (see Fig. 11d) and, again, the sign of the stresses does not change through the core's depth at the beginning of the blast and it changes at the last time step. The in-plane shear stresses at the support line are cubic (see Fig. 11e), with different signs at the various times and with different signs and values at the various face–core interfaces. The distributions of the vertical shear stresses through the depth of the core, at the supports, are cubic with a small curvature and identical signs. The signs change with time (see Fig. 11f).

The results along a section that passes through the centers of the panel and the support line ($y = b/2$) at a specific time of $t = 0.5$ ms appear in Figs. 12 and 13. The in-plane and vertical displacements of the facesheets and the core appear in Figs. 12a and 12b. The in-plane displacements in the x direction reveal different wavelengths for the core displacements. On the other hand, the vertical displacements (Fig. 12b) reveal large curvatures in the vicinity of the loaded area. The interfacial shear stresses at the face–core interfaces (see Fig. 12c) are associated with larger values in the vicinity of the edge of the loaded area, similar to a stress concentration phenomenon that occurs in a unidirectional sandwich panel loaded by a localized load (see Frostig et al. [5]). The vertical normal interfacial stresses appear in Fig. 12d, which reveals very large stresses with different values and shapes at the various interfaces. The various stress resultants appear in Fig. 13. Here, the in-plane stress resultants, in the x direction, appear in Fig. 13a, and they consist of compressive resultants in the upper facesheet and tensile ones in the lower facesheet with a small contribution from the core. Similarly, the contribution of the local bending moment stress resultants of the core (see Fig. 13b) is small as compared with those of the facesheets. The vertical shear stress resultants appear in Fig. 13c, and they are very similar to the patterns of the interfacial shear stresses (see Fig. 12c) due to the almost uniform distribution of the shear stresses through the depth of core (see Fig. 11f).

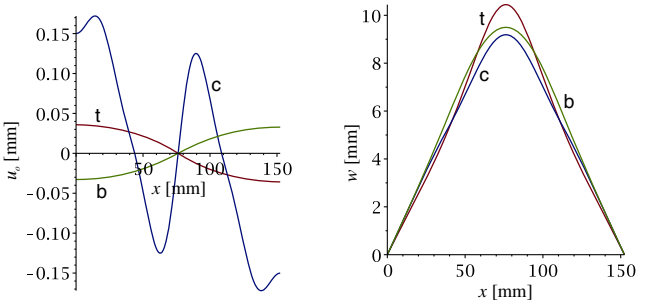

a) In-plane displacements

b) Vertical displacements

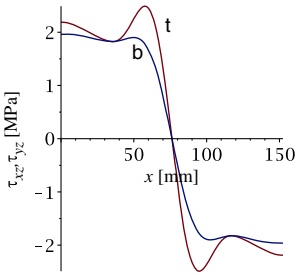

c) Interfacial shear stresses

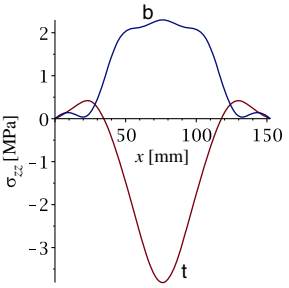

d) Interfacial vertical normal stresses

Fig. 12 Displacements of facesheets and core and interfacial stresses along section A-A (Fig. 7) of a distributed localized blast load at $t = 0.5$.

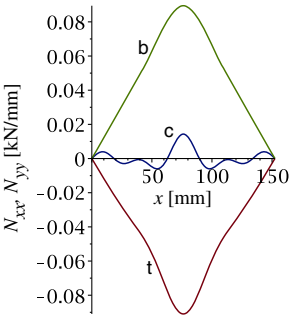

a) In-plane stress resultants

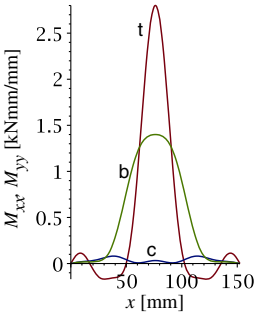

b) Bending moments stress resultants

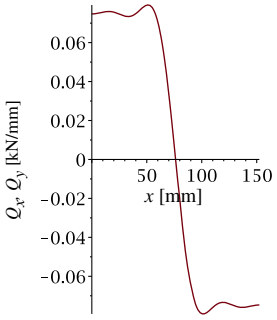

c) Core vertical shear stress resultants

Fig. 13 Stress resultants in facesheets and core along section A-A (Fig. 7) of a distributed localized blast load at $t = 0.5$.

Conclusions

A rigorous systematic analysis of the dynamic response of a sandwich plate with a compressible compliant core using the extended high-order sandwich panel theory is presented. In addition, a numerical study is conducted for a fully and locally distributed blast for a specific configuration. The mathematical formulation is based on Hamilton's principle with kinematic relations of small deformations and elastically linear materials. Notice that the equations of motion in general are valid for any type of layout of the sandwich panel and any combination of boundary conditions. In addition, it includes the high-order effects of the core along with its in-plane rigidity, in the x and y directions, through presummed cubic and quadratic distributions of the displacements with unknown functions. The proposed computational model provides a full detailed response in space and time of the various constituents of the panel.

The mathematical formulation uses Lagrange multipliers to enforce compatibility at the upper and the lower face–core interfaces, in the three directions. It includes derivation of the equations of motion along with the definition of the appropriate boundary conditions using ordinary stress resultants for the facesheets and high-order ones for the core as a result of the presumed cubic and quadratic distributions of the displacements.

The benchmark solution is a closed-form solution of the elasticity model for the case of an isotropic or orthotropic simply supported sandwich panel. The governing equations of motion are presented for the isotropic facesheets and core. They consist of a mixed set of partially differential equations and algebraic ones.

The numerical study investigates a simply supported sandwich plate with a particular setup, used for blast experiments at the University of Rhode Island (see work by Gardner et al. [24]) and subjected to a blast loading, but with some modifications. The numerical solution replaces the external loading with a Fourier series and uses the appropriate trigonometric functions to replace the partially differential equations with a set of ordinary differential equations and algebraic ones. The numerical solution is achieved using a Maple built-in DAEs solver. Two types of blast loads are considered: a fully distributed sinus pressure used for comparison with the elasticity benchmark solution, and a partially distributed blast on a small square area in the vicinity of the center of the plate.

The results, in general, include structural quantities such as displacements, stresses, and stress resultants, at specific locations, versus time and the deformed shapes of a section that passes through the center of the support line and the center of the plate, at the first millisecond at various time steps. The deformed shapes of the EHSAPT model, for the two cases, explain qualitatively yet accurately the complicated transient dynamic repose and the wave propagation involved.

In the first case, a very good correlation between the EHSAPT and the elasticity solution throughout the duration time of the investigation is observed. Up to 2 ms, a very good comparison is detected and it deteriorates with time due to the numerical damping that the numerical inverse Laplace method used in the elasticity solutions suffers from; see Kardomateas et al. [31]. The results reveal that the vertical and the in-plane displacements of the facesheets have different time periods than in the core. The in-plane displacements, in the x and y directions, of the core and its vertical normal interfacial stresses follow smaller time periods.

The second case demonstrates the effects of a localized blast load on the response. Here, the uniform distribution of the load has been replaced by a Fourier series using nine terms in each direction. The response in general follows the trends observed in the first case, but its stress patterns are erratic with small time periods and the contribution of the core relative to that of the facesheets is small. The various stress distributions, through depth of core, significantly change their shapes with time, from almost linear to nonlinear. The displacements, stresses, and stress resultants in a section that passes through the centers of the plates and the line supports reveal smooth curves with a stress concentration in the center of the plate vicinity and near the edges of the loaded region.

Finally, the paper reveals that the EHSAPT is accurate, mathematically robust, efficient, and expandable to include various sandwich panel setups; any type or combination of boundary conditions; and any type of loading schemes (dynamic, blast or static, fully loaded, or localized). In addition, due to the accurate robust solution and its ability to determine any structural quantity at any point and at any time, the physical insight is significantly enhanced. Thus, the EHSAPT should be used for the analysis of very complex responses such as the transient dynamic response of a general sandwich panel with a compliant core.

Acknowledgments

The research has been supported by the Office of Naval Research (ONR), grant N00014-11-1-0597; and the Ashtrom Engineering Company, which supports the professorship chair of Y. Frostig. The ONR Grant Monitor was Y. D. S. Rajapakse. His interest, encouragements, and the financial support received are gratefully acknowledged.

References

[1] Allen, H. G., *Analysis and Design of Structural Sandwich Panels*, Pergamon, London, 1969.
[2] Plantema, F. J., *Sandwich Construction*, Wiley, New York, 1966.
[3] Zenkert, D., *An Introduction to Sandwich Construction*, Chameleon Press, London, 1995.
[4] Vinson, J. R., *The Behavior of Sandwich Structures of Isotropic and Composite Materials*, Technomic, Lancaster, 1999.
[5] Frostig, Y., Baruch, M., Vilnai, O., and Sheinman, I., "High-Order Theory for Sandwich-Beam Bending with Transversely Flexible Core," *Journal of Engineering Mechanics*, Vol. 118, No. 5, May 1992, pp. 1026–1043. doi:10.1061/(ASCE)0733-9399(1992)118:5(1026)
[6] Carrera, E., and Brischetto, S., "A Survey With Numerical Assessment of Classical and Refined Theories for the Analysis of Sandwich Plates," *Applied Mechanics Reviews*, Vol. 62, No. 1, 2008, Paper 010803. doi:10.1115/1.3013824
[7] Pagano, N. J., "Exact Solutions for Rectangular Bidirectional Composites and Sandwich Plates," *Journal of Composite Materials*, Vol. 4, No. 1, Jan. 1970, pp. 20–34.
[8] Pagano, N. J., and Hatfield, S. J., "Elastic Behavior of Multilayered Bidirectional Composites," *AIAA Journal*, Vol. 10, No. 7, 1972, pp. 931–933. doi:10.2514/3.50249
[9] Zenkour, A. M., "Three-Dimensional Elasticity Solution for Uniformly Loaded Cross-Ply Laminates and Sandwich Plates," *Journal of Sandwich Structures and Materials*, Vol. 9, No. 3, May 2007, pp. 213–238. doi:10.1177/1099636207065675
[10] Kardomateas, G. A., "Three Dimensional Elasticity Solution for Sandwich Plates with Orthotropic Phases: the Positive Discriminant Case," *Journal of Applied Mechanics*, Vol. 76, No. 1, 2009, Paper 014505. doi:10.1115/1.2966174
[11] Kardomateas, G. A., "An Elasticity Solution for the Global Buckling of Sandwich Beams/Wide Panels with Orthotropic Phases," *Journal of Applied Mechanics*, Vol. 77, No. 2, 2010, Paper 021015. doi:10.1115/1.3173758
[12] Kardomateas, G. A., and Phan, C. N., "Three-Dimensional Elasticity Solution for Sandwich Beams/Wide Plates with Orthotropic Phases: The Negative Discriminant Case," *Journal of Sandwich Structures and Materials*, Vol. 13, No. 6, 2011, pp. 641–661. doi:10.1177/1099636211419127
[13] Srinivas, S., and Rao, A. K., "Bending, Vibration and Buckling of Simply Supported Thick Orthotropic Rectangular Plates and Laminates," *International Journal of Solids and Structures*, Vol. 6, No. 11, 1970, pp. 1463–1481. doi:10.1016/0020-7683(70)90076-4
[14] Librescu, L., Sang-Yong Oh, S.-Y., and Hohe, J., "Dynamic Response of Anisotropic Sandwich Flat Panels to Underwater and In-Air Explosions," *International Journal of Solids and Structures*, Vol. 43, No. 13, 2006, pp. 3794–3816. doi:10.1016/j.ijsolstr.2005.03.052
[15] Frostig, Y., and Baruch, M., "Free Vibration of Sandwich Beams with a Transversely Flexible Core: A High Order Approach," *Journal of Sound and Vibration*, Vol. 176, No. 2, 1964, pp. 195–208. doi:10.1006/jsvi.1994.1368
[16] Sokolinsky, V., and Frostig, Y., "High-Order Buckling of Debonded (Delaminated) Sandwich Panels with a 'Soft' Core," *AIAA Journal*, Vol. 38, No. 11, Nov. 2000, pp. 2147–2159. doi:10.2514/2.878
[17] Frostig, Y., and Thomsen, O. T., "High-Order Free Vibration of Sandwich Panels with a Flexible Core," *International Journal of Solids and Structures*, Vol. 41, Nos. 5, 6, March 2004, pp. 1697–1724. doi:10.1016/j.ijsolstr.2003.09.051
[18] Swanson, S. R., and Kim, J., "Comparison of a Higher Order Theory for Sandwich Beams with Finite Element and Elasticity Analyses," *Journal of Sandwich Structures and Materials*, Vol. 2, No. 1, 2000, pp. 33–49. doi:10.1177/109963620000200102
[19] Santiuste, C., Thomsen, O. T., and Frostig, Y., "Thermo-Mechanical Load Interactions in Foam Cored Axi-Symmetric Sandwich Circular Plates–High-Order and FE Models" *Composite Structures*, Vol. 93, No. 2, 2011, pp. 369–376. doi:10.1016/j.compstruct.2010.09.005
[20] Frostig, Y., "On Wrinkling of a Sandwich Panel with a Compliant Core and Self-Equilibrated Loads," *Journal of Sandwich Structures and Materials*, Vol. 13, No. 6, Nov. 2011, pp. 663–679. doi:10.1177/1099636211419131
[21] Phan, C. N., Frostig, Y., and Kardomateas, G. A., "Analysis of Sandwich Panels with a Compliant Core and with In-Plane Rigidity–Extended High-Order Sandwich Panel Theory Versus Elasticity," *Journal of Applied Mechanics*, Vol. 79, No. 4, July 2012, Paper 041001.
[22] Frostig, Y., Phan, C. N., and Kardomateas, G. A., "Free Vibration of Unidirectional Sandwich Panels Part I: Elasticity and High-Order Computational Models," *Journal of Sandwich Structures and Materials*, Vol. 15, No. 4, July 2013, pp. 377–411. doi:10.1177/1099636213485518
[23] Phan, C. N., Frostig, Y., and Kardomateas, G. A., "Free Vibration of Unidirectional Sandwich Panels, Part II: Incompressible Core Models and Numerical Comparisons," *Journal of Sandwich Structures and Materials*, Vol. 15, No. 4, July 2013, pp. 412–428. doi:10.1177/1099636213485520
[24] Gardner, N., Wang, E., Kumar, P., and Shukla, A., "Blast Mitigation in a Sandwich Composite Using Graded Core and Polyurea Interlayer," *Experimental Mechanics*, Vol. 52, No. 2, 2012, pp. 119–133. doi:10.1007/s11340-011-9517-9
[25] Dvorak, G. J., Bahei-El-Din, Y. A., and Suvorov, A. P., "Impact, and Blast Resistance of Sandwich Plates" *Major Accomplishments in Composite Materials and Sandwich Structures: An Anthology of ONR Sponsored Research*, edited by Daniel, I. M., Goloutos, E. E., and Rajapakse, Y. D. S., Springer Science and Business Media B.V., New York, 2009, pp. 625–659.
[26] Latourte, F., Gregoire, D., Zenkert, D., Wei, X., and Espinosa, H. D., "Failure Mechanisms in Composite Panels Subjected to Underwater Impulsive Loads," *Journal of the Mechanics and Physics of Solids*, Vol. 59, No. 8, 2011, pp. 1623–1646. doi:10.1016/j.jmps.2011.04.013
[27] Hoo Fatt, M. S., and Palla, L., "Analytical Modeling of Composite Sandwich Panels Under Blast Loads," *Journal of Sandwich Structures and Materials*, Vol. 11, No. 4, 2009, pp. 357–380. doi:10.1177/1099636209104515
[28] Li, R. F., Kardomateas, G. A., and Simitses, G. J., "Point-Wise Impulse (Blast) Response of a Composite Sandwich Plate Including Core Compressibility Effects," *International Journal of Solids and Structures*, Special Issue in Honor of Professor Liviu Librescu, Vol. 46, No. 10, 2009, pp. 2216–2223. doi:10.1016/j.ijsolstr.2009.01.036
[29] Mayercsik, N. P., "Finite Element Analysis of Advanced Composite Sandwich Panel Core Geometries for Blast Mitigation," B.C.E. Thesis, Civil and Environmental Engineering, Univ. of Delaware, Newark, DE, 2010.
[30] Char, B. W., Gedddes, K. O., Gonnet, G. H., Leong, B. L., Monagan, M. B., and Watt, S. M., *Maple V Library Reference Manual*, Springer–Verlag, New York, 1991.
[31] Kardomateas, G. A., Rodcheuy, N., and Frostig, Y., "Transient Blast Response of Sandwich Plates by Dynamic Elasticity," *AIAA Journal* [online], Jan. 2015. doi:10.2514/1.J052865

S. Pellegrino
Associate Editor